Supplemental Materials

Molecular Biology of the Cell

Yamashiro et al.

New single-molecule speckle microscopy reveals modification of the retrograde actin flow by focal adhesions at nanometer scales

Sawako Yamashiro, Hiroaki Mizuno, Matthew B. Smith, Gillian L. Ryan, Tai Kiuchi, Dimitrios Vavylonis & Naoki Watanabe

Supplementary figure legend

Supplementary figure S1 Expression of mRFP1-actin affects the speed of an FH1-FH2 domain fragment of mDia1 in XTC cells. Displacement of processively moving (>1 s) EGFP-mDia1ΔN3 speckles in two control cells (A, n = 24 speckles; B, n = 17) and 5 cells expressing mRFP1-actin. The cell expressed mRFP1-actin at a very low level (C, n = 37), low levels (D, n = 21; E, n = 21), a high level (F, n = 29) and a very high level (G, n = 15). (B-G) Insets indicate expression of mRFP1-actin. Bars: 10 μm.

Supplementary figure S2 Gel filtration with Superdex 200 enriches single DyLight (DL)-labeled actin. (A) Elution profile of DL549-labeled actin by gel filtration. After labeling F-actin with DyLight549 NHS-ester, actin was depolymerized in G-buffer (see Materials and Methods) and loaded on a Superdex 200. (B) MALDI-TOF mass spectrometry profiles of control unlabeled actin and DL-actin fractions 1-3 in (A). DL-actin in each fraction was mixed with sinapinic acid solution (10 mg mL^{-1} in 30% acetonitrile and 0.1 % trifluoroacetic acid), and analyzed with a 5800 MALDI-TOF mass spectrometer (Applied Biosystems). Expected mass of actin (grey break line) and those of actin labeled with 1 to 4 DL549 (orange break lines) are indicated. DL-actin fractions were detected as broad peaks, presumably representing the peaks of actin labeled with varied numbers of DL dye(s). The broad peak of the fraction 1 corresponds to the estimated mass of actin labeled with two dyes (43,551 Da) and three dyes (44,418 Da),

suggesting that major species of actin in the fraction were double or triple DL-actin. On the other hand, the peaks of the fractions 2 and 3 shifted to smaller mass than the peak of the fraction 1 gradually, suggesting that single DL-labeled actin was enriched to the fractions 2 and 3. Since the peak of the fraction 2 tailed and the fraction probably contained double and triple DL-actin as a major part, we used the fraction 3 for all experiments. The labeling efficiencies for the fractions, which were calculated by the absorbance of DL-actin at 290 nm for actin and 562 nm for DL549 dye, were 44% for the fraction 1, 21% for the fraction 2 and 12% for the fraction 3. According to the labeling efficiencies, the fractions 1 and 2 should contain 56% and 79% of unlabeled actin, respectively. However, unlabeled actin was not detected with adequate ratios to labeled actin in the mass spectrometry profiles of the fractions 1 and 2. This discrepancy might be explained by the two possibilities: i) A fraction of DL549 might become incapable of absorbing 562 nm light. ii) DL-labeled actin might have been ionized more efficiently than unlabeled actin and detected dominantly in the mass spectrometry analysis.

Supplementary figure S3 Incorporation of DL549-actin into formin-associated actin filaments *in vitro*. Additional data observed by direct observation of formin-mediated actin assembly *in vitro*. (A) Time-lapse images of actin assembly with 1 μM OG_{Cys374}-actin, 3 μM profilin and 7.5 nM GST-FMNL2 (FH1FH2) on glass coverslips coated with NEM-myosin II. Red arrows indicate the formin-free barbed ends, and blue arrows indicate the barbed ends undergoing FMNL2 (FH1-FH2) associated growth. (B) Kymograph shows the length (*y*-axis) of filament in (A) versus time (*x*-axis). Blue arrows indicate association (ON) of GST-mDia1ΔN3 or mDia2 (FH1FH2), and red arrows indicate dissociation (OFF) of formins. Arrows indicate as in Figure 1A and B. (C) Time lapse images of DL488-actin filaments growing from mDia1ΔN3 attached to the glass

surface (filament 1) or growth of a spontaneously assembled filament (filament 2). P: pointed ends. B: barbed ends. (D) Kymograph shows the length (*y*-axis) of filament 1 in (C) versus time (*x*-axis). (E) Time lapse images of DL549-actin filaments growing from FMNL2 (FH1-FH2) attached to the glass surface (filament 1) or a growth of spontaneously assembled filament (filament 2). P: pointed ends. B: barbed ends.

Supplementary figure S4 One-step photobleaching of DL549-actin speckles in fixed cells. XTC cells loaded with DL549-actin by electroporation were fixed with 70% PBS containing 3.7 % paraformaldehyde and 0.2 % Triton X-100 for 10 min, and then the chamber was filled with the L15 medium without a serum and rivoflavin. Images were acquired at 100 ms intervals under continuous illumination with unattenuated 100W mercury-arc lamp. (A) DL549-actin in LP of XTC cells loaded with DL549-actin by electroporation. (B) Fluorescence intensity of 12 individual speckles in the boxed area in (A). (C) Fluorescence intensity in the background areas devoid of speckles. The circular regions with the same size were used for measuring fluorescence intensity of DL-actin speckles (B) and the background (C). Sudden, one-step decrease of the intensity to the background level (C) occurred with all DL-actin speckles.

Supplementary figure S5 (A) Images of DL-actin speckles and fluorescent organelle-like structures (pink arrows). (B) Time-lapse images of a fluorescent organelle-like (pink arrows) in the rectangle area in (A). The fluorescent organelle-like structures are easily distinguishable from single-molecule speckles by their size, brightness and random movement.

Supplementary figure S6 **(**A and B) Examples of FRAP of DL488-actin speckles on LP of XTC cells. We performed FRAP of DL488-actin with the 435 nm laser. The cells expressing mCherry-actin were used to monitor the actin structures, and DL488-actin was delivered into the cells by electroporation. DL488-actin was photobleached with twenty times of 435 nm laser pulses using the MicroPoint laser system (Photonic Instruments). The photobleached regions are indicated by white lines. Typically, the region contained 4-10 speckles before photobleaching. Multiple DL488-actin speckles reappeared in the bleached region within 30 seconds after photobleaching, which was reproducibly observed (14/17 experiments, 9 cells). To photobleach DL488-actin, we had to use a strong irradiation condition. Under the condition, mCherry-actin was also partly bleached by 435 nm laser, which conveniently marked photobleached regions. The photobleached regions of mCherry-actin showed that the retrograde flow remained largely constant after irradiation. These results suggest rapid actin turnover in LP of XTC cells. (C) Speed and trajectory maps of DL488-actin speckles before and after photobleaching for Cell 1 (upper) and Cell 2 (lower). Although the retrograde flow remained after photobleaching, the flow speeds were slightly decreased after photobleaching in some cells as in Cell 2. (D) Recovery of DL488-actin speckles after photobleaching. Total numbers of speckles (blue bars), newly appeared speckles (pink bars) and disappeared speckles (green bars) from the preceding image are shown. After photobleaching, speckles reappeared and thereby the number of total speckles increased immediately after bleaching within 6 sec. And then, the number of speckles remained almost constant. Speckles (10 to 30%) newly appeared and disappeared constantly, suggesting that rapid actin turnover occurred in the region. Note that photobleaching rate was less than 20% under the imaging condition.

Supplementary figure S7 Nanometer displacement measurements of DL549-actin

speckles in lamellipodia. The data show other examples of the experiments in Fig. 5D. The velocity of all measureable speckles is plotted as a function of distance from the cell edge. Each graph shows the data of distinct cells (Cells 2-5). Pink dots indicate short-lived speckles that appeared and disappeared in10 seconds.

Supplementary figure S8 Effects of mature FAs on the local actin retrograde flow in lamellipodia. The data show other examples of the experiments in Fig. 6. (A and C) Average speed and trajectory maps of DL-actin speckles in LP containing mature FAs. Lines indicating the trajectories and speeds of DL549-actin speckles observed within a 300 seconds time window as in Figure 6A. (C and D) Local speed and trajectory maps of DL-actin speckles in the boxed region in A and B. Local actin flow speeds were measured with a 15 second time window (3 frames). The circles indicate the position of individual speckles in the second frame of the three, and their color indicates the local speed of the speckle. Circles from the data of a single speckle are linked with gray lines in sequences of frames. (E) The speckle data of 8C are divided into three time windows (0-100 s, 101-200 s and 201-300 s). Note that in this particular cell, the actin flow rate changed globally in LP over time. The actin flow rate in LP appears to fluctuate in XTC cells on rare occasions. Similar observation has been reported in PtK1 epithelial cells (Burnette *et al.*, *Nat Cell Biol.*, 13, 371-381, 2011). Nevertheless, in each time window, actin speckles in front of the FA moved toward the FA with similar speeds to those of surrounding speckles. Bars: 5 μm

Supplementary figure S9 In Figure 6B, the indicated regions I-III in Cells 1-3 were used to compare regional actin flow speeds in LP between the location in front of FAs (I of Cell 1 and Cell 2, I and II of Cell 3) and apart form FAs (II and III of Cell 1 and Cell 2,

III of Cell 3).

Supplementary Movie legends

Movie 1 Elongation of OG_{Cys374}-actin filament (left) and DL549-actin filament (right) attached to the glass surface by NEM-myosin II at 1 μM G-actin, 3 μM profilin and 1 nM GST-mDia1ΔN3 (Fig. 1A and C). Time is given in seconds. Scale bar, 5 μm.

Movie 2 Elongation of OG_{Cys374}-actin filament (left) and DL549-actin filament (right) attached as Movie1 at 1 μM G-actin, 3 μM profilin and 7.5 nM GST-mDia2 (FH1-FH2) (Fig. 1E and G). Time is given in seconds. Scale bar, 5 μm.

Movie 3 Elongation of dim DL549-actin filaments from GST-FMNL2 (FH1-FH2) immobilized on the glass surface (arrows). The dim filaments occasionally detached from the glass surface for a short time, which was correspond to elongation of bright segments from free barbed ends. Time is given in seconds. Scale bar, 5 μm.

Movie 4 Time-lapse movie of an XTC cell that DL549-actin was microinjected into (Fig. 2A). Time is given in minutes and seconds. Scale bar, 5 μm.

Movie 5 Time-lapse movie of single-molecule speckles of DL549-actin in LP acquired at intervals of 6 s. DL549-actin was delivered into the XTC cell by electroporation (Fig. 2B). Time is given in minutes and seconds. Scale bar, 5 μm.

Movie 6 Time-lapse movie of an XTC cell expressing Lifeact-mCherry at intervals of 30 s (Fig. 4A). Fifty μM blebbistatin was added between 10 min and 10 min 30 s. Time is

given in minutes and seconds. Scale bar, 5 μm.

Movie 7 Time-lapse movie of single-molecule speckles of DL549-actin acquired at intervals of 6 s. Fifty μM blebbistatin was added between 3 min 30 s and 3 min 48 s. Time is given in minutes and seconds. Scale bar, 5 μm.

Movie 8 Time-lapse movie of single-molecule speckles of DL549-actin (red) acquired at intervals of 2 s (Fig. 6A, mature FA). The movie is overlaid with an image of EGFP-vinculin (green) before acquisition of the SiMS imaging for DL549-actin. Time is given in minutes and seconds. Scale bar, 5 μm.

Movie 9 Time-lapse movie of single-molecule speckles of DL549-actin (red) acquired at intervals of 2 s (Fig. 7A, nascent FAs). The movie is overlaid with an image of EGFP-vinculin (green) before acquisition of the SiMS imaging for DL549-actin. Time is given in minutes and seconds. Scale bar, 5 μm.

Movie 10 Time-lapse movie of single-molecule speckles of DL549-actin (red) acquired at intervals of 10 s (right) and the local speed and trajectory map of speckles in the movie (left) (Supplementary Fig. S8A and C, Cell2). The movie is overlaid with an image of EGFP-vinculin (left, gray scale; right, green) before acquisition of the SiMS imaging for DL549-actin. Time is given in seconds. Scale bar, 5 μm.

Movie 11 Time-lapse movies of FRAP of DL488-actin (top left) acquired at intervals of 3 s (Supplementary Fig. S6A). DL488-actin was photobleached between -3 s and 0 s. Top right: mCherry-actin. Bottom left: merged movie. The photobleached region is indicated

by white lines in the merged movie. Scale bar, 5 μm.

Suppl Fig. 1

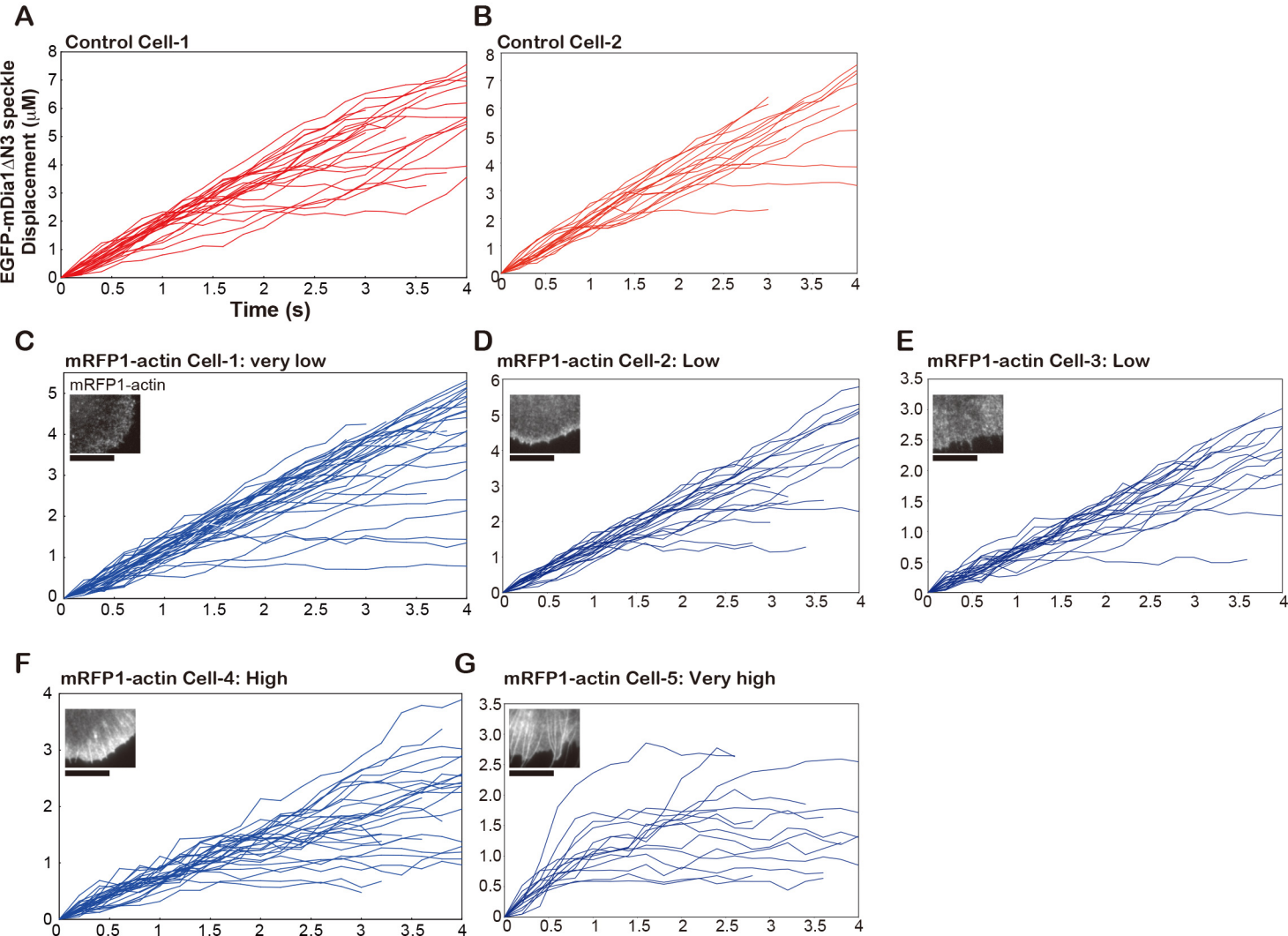
A
Control Cell-1
EGFP-mDia1ΔN3 speckle Displacement (μM)
Time (s)
B
Control Cell-2
C
mRFP1-actin Cell-1: very low
mRFP1-actin
D
mRFP1-actin Cell-2: Low
E
mRFP1-actin Cell-3: Low
F
mRFP1-actin Cell-4: High
G
mRFP1-actin Cell-5: Very high

Suppl Fig. 2

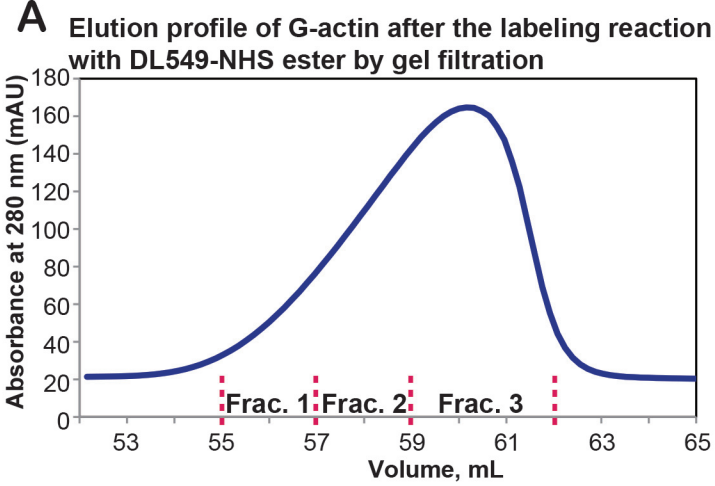
A
Elution profile of G-actin after the labeling reaction with DL549-NHS ester by gel filtration
Absorbance at 280 nm (mAU)
180
160
140
120
100
80
60
40
20
0
Frac. 1
Frac. 2
Frac. 3
53
55
57
59
61
63
65
Volume, mL

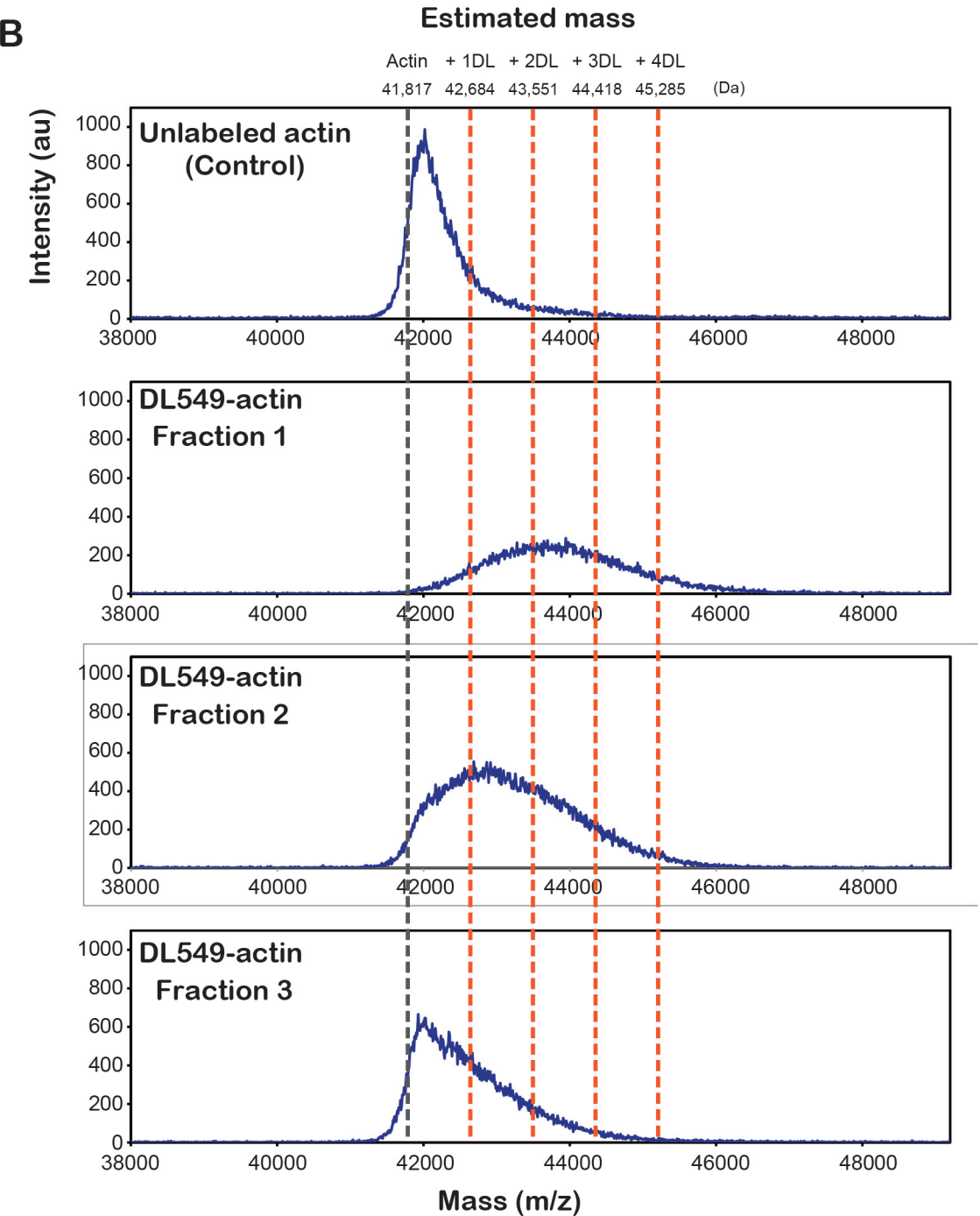
B
Estimated mass
Actin + 1DL + 2DL + 3DL + 4DL
41,817 42,684 43,551 44,418 45,285 (Da)
Intensity (au)
Unlabeled actin (Control)
DL549-actin Fraction 1
DL549-actin Fraction 2
DL549-actin Fraction 3
1000
800
600
400
200
0
38000
40000
42000
44000
46000
48000
Mass (m/z)

Suppl Fig. 3

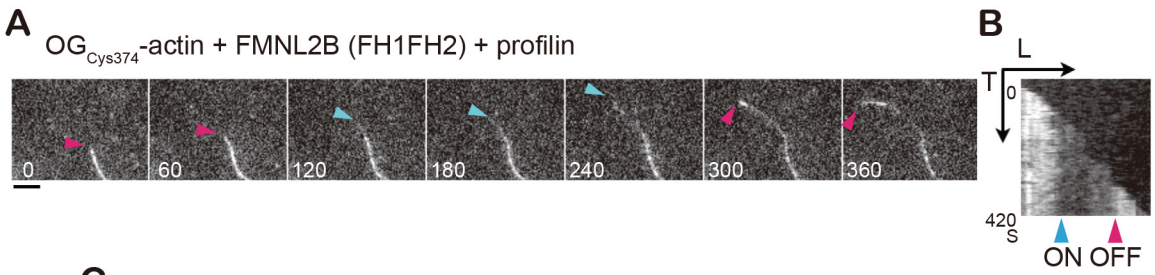

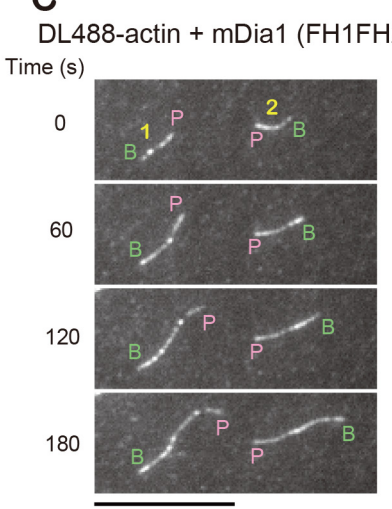

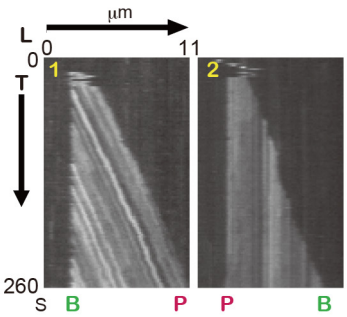

1: formin FH1-FH2 associated filament

2: native filament

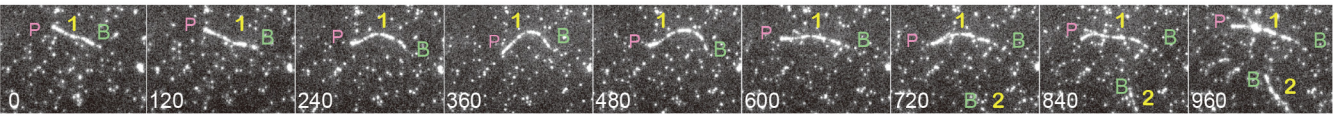

Suppl Fig. 4

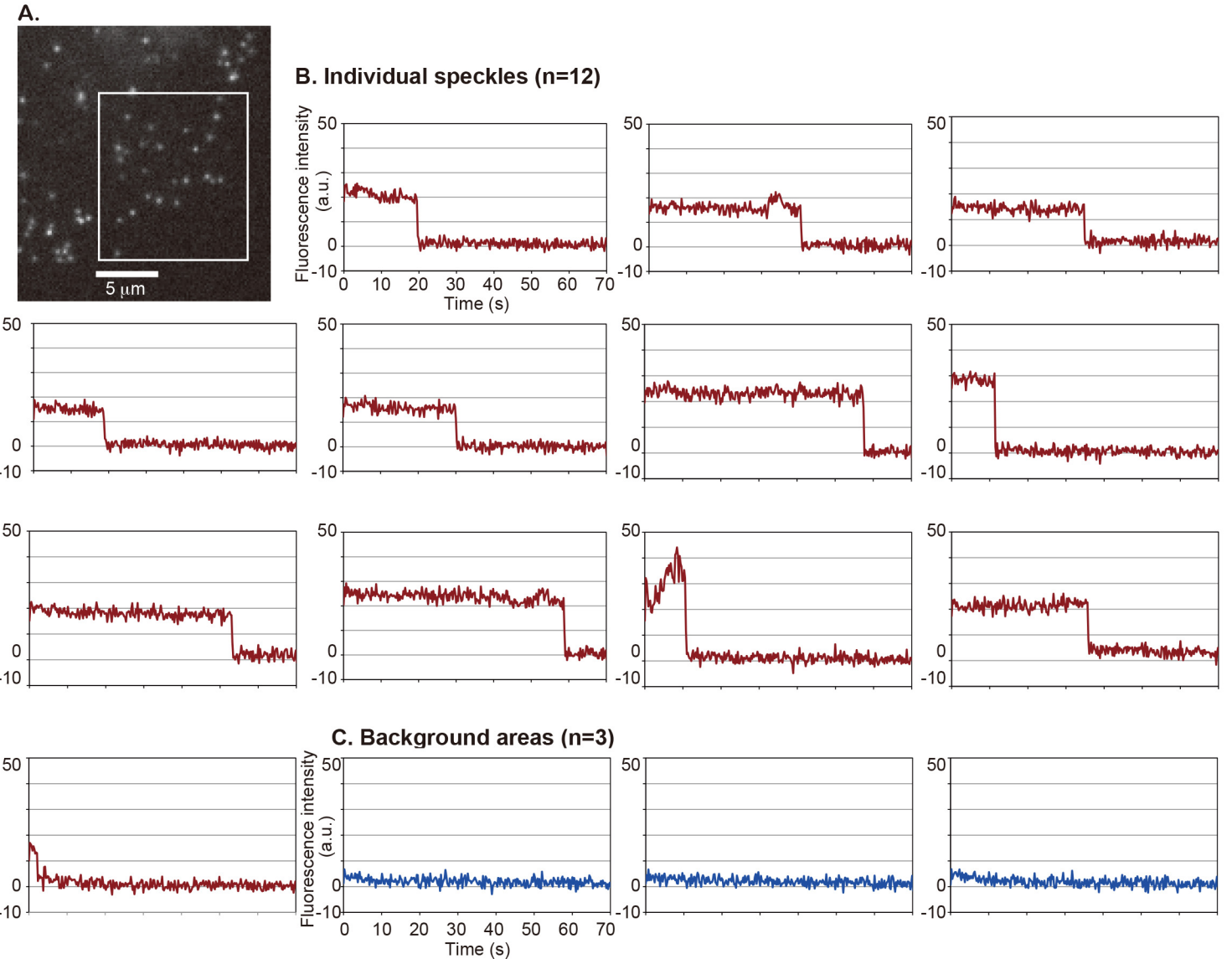
A.
5 µm
B. Individual speckles (n=12)
Fluorescence intensity (a.u.)
50
0
-10
0 10 20 30 40 50 60 70
Time (s)
C. Background areas (n=3)
Fluorescence intensity (a.u.)
Time (s)

Suppl Fig. 5

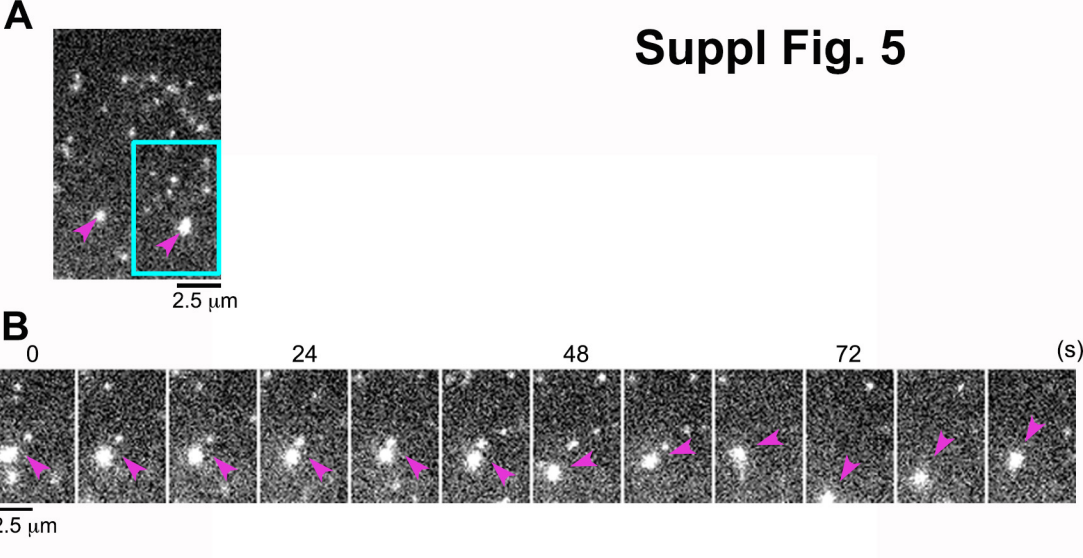

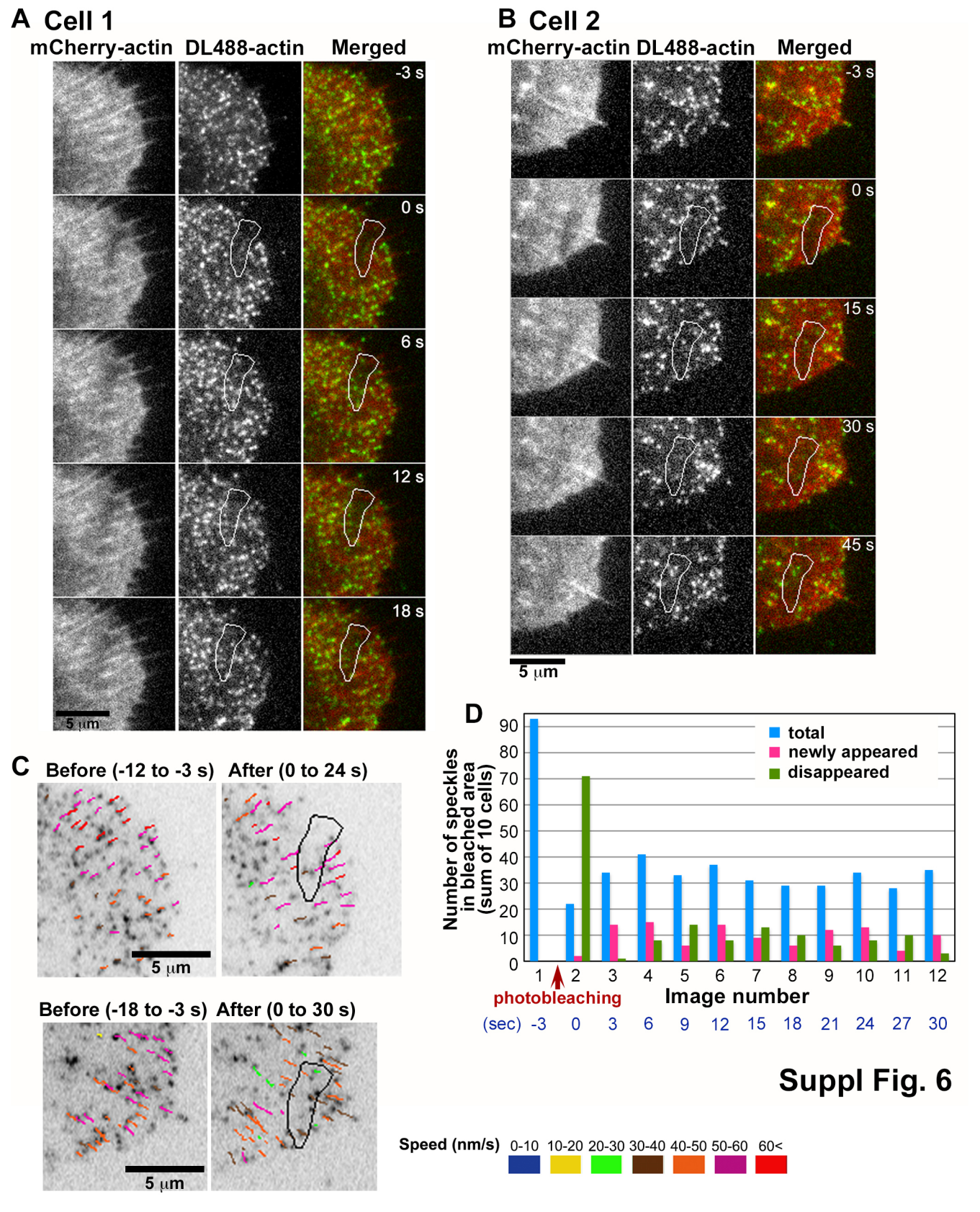
A Cell 1
mCherry-actin
DL488-actin
Merged
-3 s
0 s
6 s
12 s
18 s
5 μm
B Cell 2
mCherry-actin
DL488-actin
Merged
-3 s
0 s
15 s
30 s
45 s
5 μm
C
Before (-12 to -3 s)
After (0 to 24 s)
5 μm
Before (-18 to -3 s)
After (0 to 30 s)
5 μm
D
Number of speckles in bleached area (sum of 10 cells)
total
newly appeared
disappeared
photobleaching
Image number
(sec) -3 0 3 6 9 12 15 18 21 24 27 30
Speed (nm/s)
0-10
10-20
20-30
30-40
40-50
50-60
60<
Suppl Fig. 6

Suppl Fig. 7

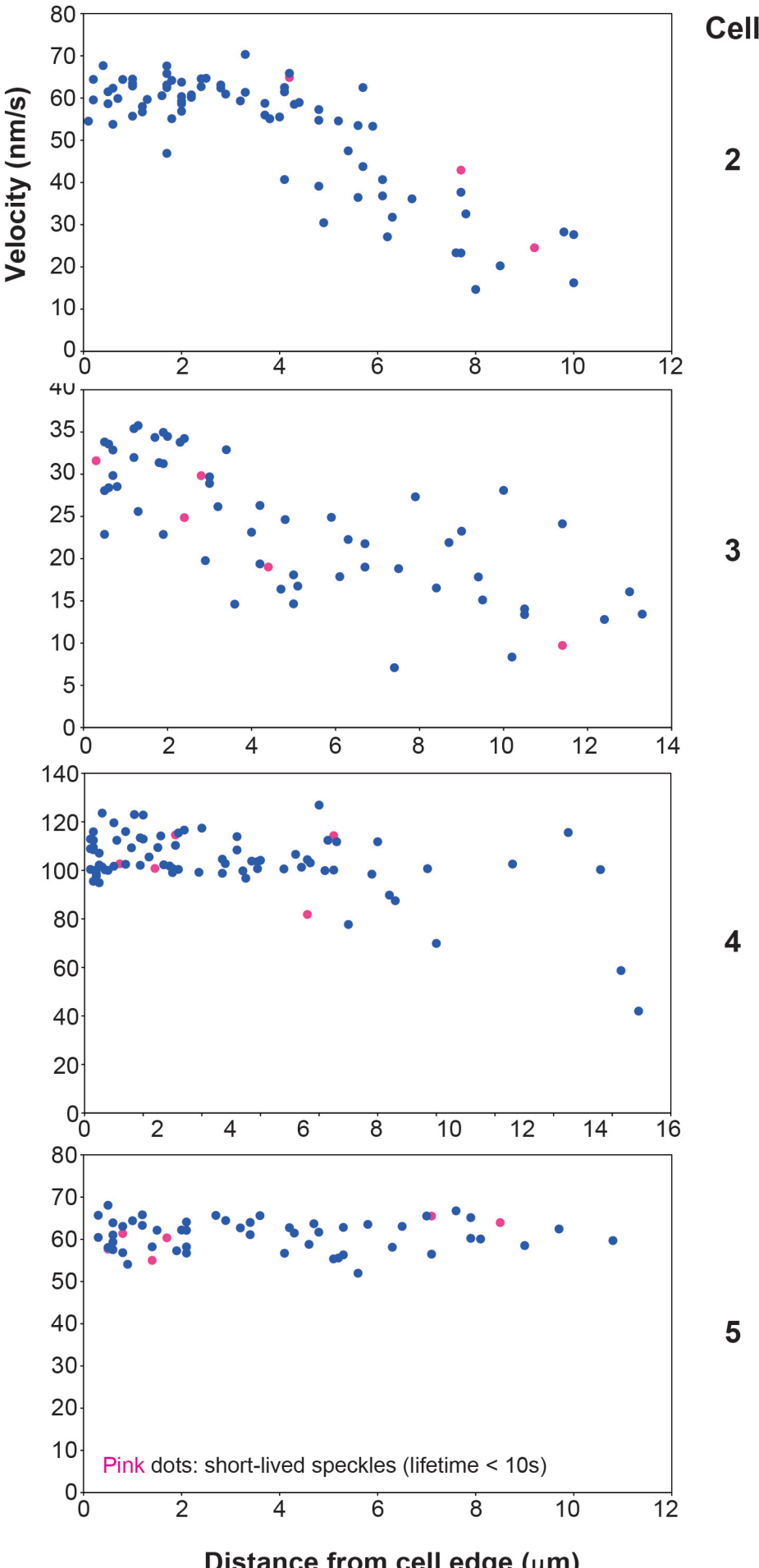
Cell
2
3
4
5
Velocity (nm/s)
Pink dots: short-lived speckles (lifetime < 10s)
Distance from cell edge (μm)

Suppl Fig. 8

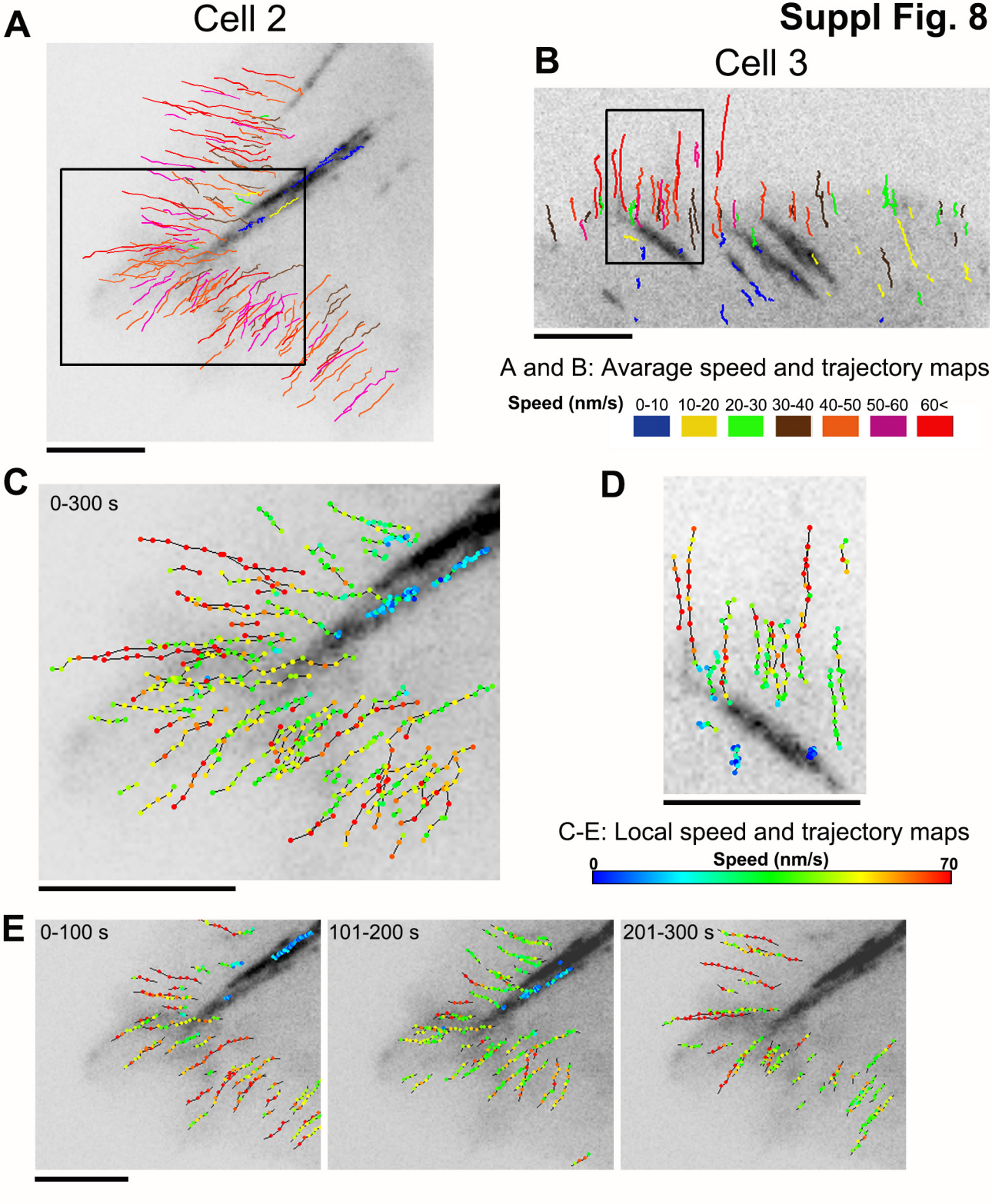
A
Cell 2
B
Cell 3
A and B: Avarage speed and trajectory maps
Speed (nm/s)
0-10
10-20
20-30
30-40
40-50
50-60
60<
C
0-300 s
D
C-E: Local speed and trajectory maps
0
Speed (nm/s)
70
E
0-100 s
101-200 s
201-300 s

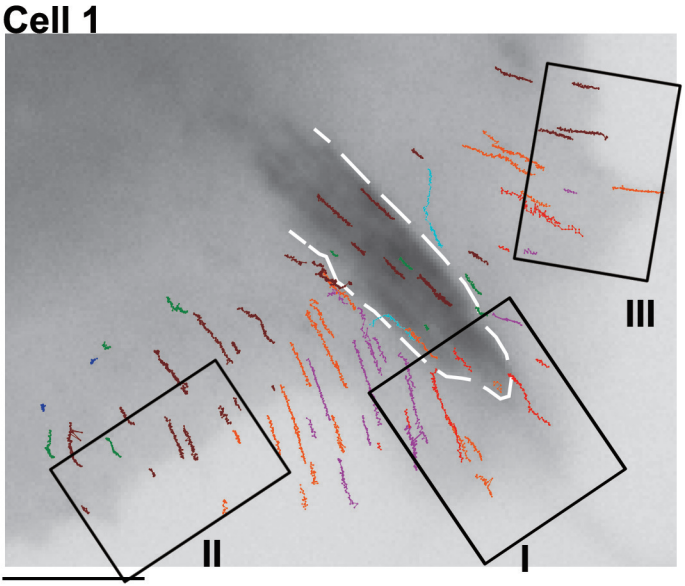

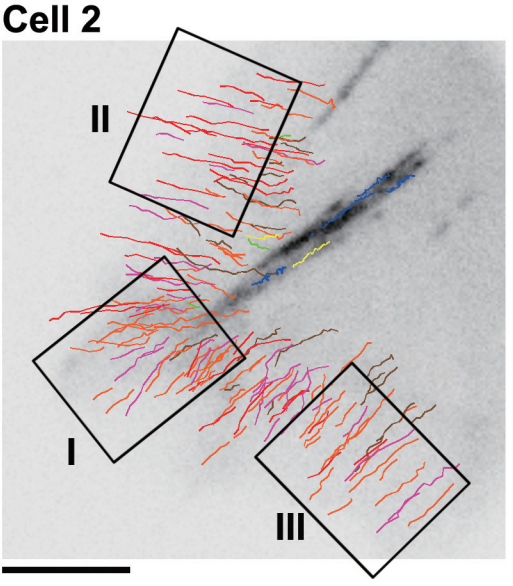

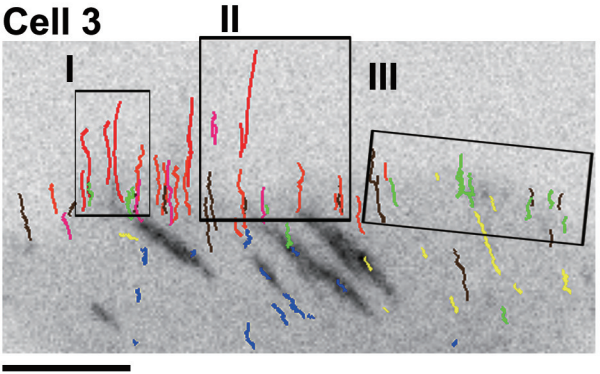

Suppl Fig. 9